ABSTRACT

AMANDA L. DYE: Lattice Boltzmann Simulation of Non-Darcy Flow in Sphere Packings
(Under the direction of Dr. Cass T. Miller.)

Lattice-Boltzmann modeling was used to simulate single-phase, non-Darcy flow through flow domains constructed utilizing an algorithm that supports the generation of a system of spheres with log-normally distributed radii and a defined porosity. Representative elementary volumes were determined using the permeability and inertial coefficients of a non-dimensional momentum equation for a range of sphere-size distributions. Porous media were generated for porosities ranging from 0.3 to 0.6 for the different sphere-size distributions. The parameters obtained from the non-Darcy flow model did not fit the existing permeability and inertial correlations proposed by Carmen-Kozeny, Rumpf-Gupte, Ergun and others. Based on the experimental data collected from the lattice-Boltzmann simulations, empirical correlations are suggested that relate the permeability and inertial parameters with the porosity.

ACKNOWLEDGMENTS

First I want to thank my advisor Dr. Miller and Dr. Gray for taking a chance on me. I deeply appreciate their patience and contributions of time, ideas, and funding to make my Masters experience both productive and stimulating. I would also like to thank Dr. Vizuete for taking the time to be on my thesis committee.

I am forever indebted to James McClure for all the long-suffering he had to go through to help me understand the programming side of my research. He authored much of the coding that went into making this work possible and took on the unofficial role of problem fixer along the way.

I am also grateful to Sarah Shelton for all the emotional support, help, and comraderie she has provided throughout this sometimes difficult process.

Lastly, I would like to thank my family for all their love and encouragement. For my siblings, Samantha, Erica, and Kevin, my papa, Bill, who has been my biggest fan since the beginning, always inspiring me to follow my dreams, and most of all my parents, Bill and Pam, who have been a constant source of support - emotional, moral, and of course financial - throughout my student career and this thesis would certainly not have existed without them. It is thanks to the two of them for exposing me to the world and igniting my ongoing search for knowledge -it is to them, my role models, this thesis is dedicated.

TABLE OF CONTENTS

LIST OF TABLES

Table

LIST OF FIGURES

Introduction

Single phase flow in porous media plays a fundamental role in many natural and industrial processes. While the primary approaches for describing these systems are rooted in empiricism, recent work has focused on deriving traditional models for single phase flow from first principles and linking macroscopic phenomena with microscale flow behavior (Hassanizadeh and Gray, 1987, 1988; Ma and Ruth, 1994) . The current state of knowledge categorizes single phase flow into two primary regimes: a weak inertia regime corresponding to small flow velocities in which viscous forces completely dominate inertial forces and a strong inertia regime corresponding to moderate flow velocities in which inertial forces can not be neglected (Ma and Ruth, 1994; Wang, Thauvin and Mohanty, 1999; Fourar et al., 2004; Panfilov and Fourar, 2006). These two regimes are linked to two of the most commonly applied models, Darcy's law and the Forchheimer equation.

State of the art numerical methods provide the opportunity to study flow in porous media directly from the microscale. This provides the opportunity to assess details of the microscale flow structure in addition to macroscopic forms. The lattice Boltzmann method has gained popularity for simulation of porous media and other complex systems due to computational advantages over more traditional fluid dynamics approaches, particularly in handling complex boundary conditions and parallelization. Multi Relaxation Time (MRT) lattice Boltzmann schemes have been demonstrated to have many advantages over the more widely used single relaxation time (BGK) lattice Boltzmann model, including improved numerical stability and simulation of high Reynolds number flows (Pan, Luo and Miller, 2006).

The overall goal of this work is to advance the understanding of single fluid phase flow by performing microscale flow simulations using the lattice Boltzmann method. Isotropic porous medium systems will be considered for Reynolds numbers ≤ 150. The specific objectives of this work are:

1. to investigate the most appropriate form of approximate momentum equations; and
2. to develop relations to estimate momentum equation parameters from porous medium characteristics.

Background

Darcy's law for one-dimensional flow in porous medium can be expressed in the form (Gray and Miller, 2006):

$$-\frac{\partial p^w}{\partial x} + \rho^w g_x^w = \epsilon \hat{R} v_x^w, \tag{1}$$

where p^w is the macroscale fluid pressure, ρ^w is the macroscale fluid density, $g_x^\oplus$ is the external force per unit mass acting on the fluid phase in the x direction, ϵ is the porosity, $v_x^\oplus$ is the barycentric macroscale velocity of the fluid relative to the solid in the x direction, and $\hat{R}$ is the momentum resistance coefficient. The form of $\hat{R}$ is of principle concern for the study of flow in porous media, and is known to depend on properties of the porous medium and fluid as well as the Reynolds number:

$$Re = \frac{\rho^w v_x^\oplus d}{\hat{\mu}^w}, \tag{2}$$

where $\hat{\mu}^w$ is the dynamic viscosity and d is a characteristic pore length scale. For flows in which inertial forces may not be neglected, the momentum resistance coefficient can be approximated by (McClure, Gray and Miller, 2010):

$$\hat{R} = \frac{\hat{\mu}^w}{\epsilon d^2}\left[\hat{a}\left(\mathfrak{M}\right) + \hat{b}\left(\mathfrak{M}\right)|Re|\right]. \tag{3}$$

The coefficient $\hat{a}$ is related to the intrinsic permeability of the porous medium and $\hat{b}$ relates to the strength of inertial effects. These coefficients provide a macroscopic measure of the influence that porous medium morphology and topology exert on microscopic flow behavior, and are therefore presumed to depend on an unknown set of dimensionless morphological measures $\mathfrak{M}$. Identification of an appropriate set of measures permits the construction of predictive constitutive laws, an objective which has been pursued extensively by other authors (Tek, 1957; Geertsma, 1974).

In order to simplify subsequent analysis, a dimensionless form for the momentum equation can be constructed by substituting Eq. 3 into Eq. 1 and multiplying by $\rho^w d^3/\left(\hat{\mu}^w\right)^2$ to obtain:

$$Fo = \left[\hat{a}\left(\mathfrak{M}\right) + \hat{b}\left(\mathfrak{M}\right)|Re|\right] Re, \tag{4}$$

where the dimensionless forcing term is defined as:

$$Fo = \frac{\rho^w d^3}{\left(\hat{\mu}^w\right)^2}\left(-\frac{\partial p^w}{\partial x} + \rho^w g_x^\oplus\right). \tag{5}$$

The most significant aspects of porous medium morphology with respect to prediction of the coefficients $\hat{a}$ and $\hat{b}$, are the porosity ϵ and the specific surface area ϵ^s. Surface-to-volume ratio plays a key role in microscopic flow processes, and its effect can be incorporated into the dimensionless flow equations by relating its value to the length scale for the system:

$$d = 6\frac{(1-\epsilon)}{\epsilon^s}. \tag{6}$$

The length defined by Eq. 6 is the diameter of the sphere with the equivalent surface-to-volume ratio, typically known as the Sauter diameter.

With the effects due to the specific surface area accounted for by the length scale definition, existing correlations typically predict the coefficient values $\hat{a}$ and $\hat{b}$ as functions of the porosity only. The most well-known of these expressions is Ergun's equation, which specifies functional forms for the dimensionless permeability:

$$\frac{1}{\hat{a}} = \frac{\kappa}{D^2} = A\frac{(1-\epsilon)^2}{\epsilon^2}, \tag{7}$$

and inertial coefficient:

$$\hat{b} = B\frac{(1-\epsilon)}{\epsilon}. \tag{8}$$

When these expressions are compared to those associated with the volumetric flow rate, use of the Reynolds number as defined by Eq. 2 accounts for a difference of $1/\epsilon$ in the permeability expression and $1/\epsilon^2$ in the expression for the inertial coefficient. Ergun suggested that $A = 150$ and $B = 1.75$ (Ergun, 1952), but several different values for the coefficients have been proposed. When $A = 180$, Eq. 7 is the widely used Carmen-Kozeny relationship (Bear, 1972). MacDonald et. al. determined a range for the B coefficient, $1.8 \leq B \leq 4.0$, that served to match experimental data from six different porous medium models (Macdonald F., 1979). Other correlation forms have been proposed additionally to these modified Ergun forms.

For the case of Darcy flow, Rumpf and Gupte predict the permeability using the relationship (Rumpf and Gupte, 1971):

$$\frac{\kappa}{D^2} = \frac{1}{5.6}\epsilon^{5.5}. \tag{9}$$

Pan et. al. found that the Carmen-Kozeny relationship underestimates the permeability, and observed deviations from the Rumpf-Gupte relation when systems outside the range of experimental support for this expression were considered. They proposed an alternative correlation form in which an additional dimensionless variable, the relative standard deviation $\tilde{\sigma}_D$, was also included (Pan, Hilpert and Miller, 2001):

$$\frac{\kappa}{D^2} = \beta_1\epsilon^{\beta_2}(1 + \beta_3\tilde{\sigma}_D^{\beta_4}). \tag{10}$$

More generally, the coefficients in Eq. 4 may depend upon any independent, dimensionless measure of porous medium morphology. For the case of flow in heterogeneous, isotropic media composed of sphere packings, we presume that the flow may be described adequately by assuming dependencies of the form:

$$\hat{a}(\mathfrak{M}) \approx \hat{a}_1(\epsilon)\hat{a}_2(\tilde{\sigma}_D), \tag{11}$$

$$\hat{b}(\mathfrak{M}) \approx \hat{b}_1(\epsilon)\hat{b}_2(\tilde{\sigma}_D), \tag{12}$$

where:

$$\tilde{\sigma}_D = \frac{\left[\left(e^{\sigma^2}-1\right)e^{2\mu+\sigma^2}\right]^{1/2}}{d}, \tag{13}$$

in the case that the radii are log-normally distributed with mean μ and variance σ^2.

Methods

Generation of Media

Surrogate porous media were constructed utilizing a collective rearrangement algorithm that generates sphere packings with log-normally distributed radii and a defined porosity. The algorithm is based on one used by Williams and Philipse to generate packings of sphereocylinders (Williams and Philipse, 2003) and follows these major steps:

1. A system containing a set number of spheres of the specified variance is constructed within the allocated domain
2. Overlaps between the spheres are eliminated
3. The size of the radii is increased by a constant factor

Steps 2 and 3 are repeated until the system of packed spheres reaches the desired porosity. By initializing and rescaling the radii in an appropriate way, sphere packings may be generated with log-normally distributed radii:

$$\log\left(r^{(i)}\right) \sim \text{Normal}(\mu, \sigma^2). \tag{14}$$

The variance σ^2 is provided as an input parameter while the mean μ is determined by the final packing porosity.

To accelerate convergence, the system of spheres is divided into a set of cells each composed of equally-sized subdomains. Each of the cells contains a list of the spheres with centroids located within the boundaries of the cell. For any given sphere overlaps are only considered from the neighboring cell, therefore the algorithm runtime is accelerated by increasing the number of cells because the length of the search path when computing overlaps is decreased. To prevent oversights in the overlap computation in the event the maximum sphere radius exceeds one half the cell width, the maximum radius is checked after the simulation is complete and a warning message is issued by the program if the maximum radius is too large for the specific cell width.

Multi-Relaxation Time Lattice Boltzmann Scheme

In this work, we utilize a three-dimensional, nineteen velocity vector (D3Q19) multi-relaxation time (MRT) formulation of the lattice Boltzmann method to obtain steady state velocity fields for a sequence of Reynolds numbers. In this approach, a solution for the pore-scale velocity field $\mathbf{u}(\mathbf{x}_i)$ is obtained at evenly space lattice sites $\mathbf{x}_i$ by considering the evolution of a set of discrete distributions $f_q(\mathbf{x}_i)$, where the index q is associated with a particular discrete velocity:

$$\boldsymbol{\xi}_q = \begin{cases} \{0,0,0\}^T & \text{for } q = 0 \\ \{\pm 1,0,0\}^T, \{0,\pm 1,0\}^T, \{0,0,\pm 1\}^T & \text{for } q = 1,2,\ldots,6 \\ \{\pm 1,\pm 1,0\}^T, \{\pm 1,0,\pm 1\}^T, \{0,\pm 1,\pm 1\}^T & \text{for } q = 7,8,\ldots,18. \end{cases} \tag{15}$$

The density and momentum can be expressed as linear combinations of the discrete distributions:

$$\rho = \sum_{q=0}^{18} f_q, \tag{16}$$

$$\mathbf{u} = \frac{1}{\rho^o} \sum_{q=0}^{18} \boldsymbol{\xi}_q f_q. \tag{17}$$

Within the MRT framework, the relaxation of the discrete distributions toward their equilibrium values is modeled by considering a set of equilibrium moments $\hat{f}_m$ obtained by a linear transformation of the distributions:

$$\hat{f}_m = \sum_{0}^{18} M_{m,q} f_q. \tag{18}$$

The values transformation matrix $M_{m,q}$ are chosen based on a Gram-Schmidt orthogonalization constructed using polynomials of the discrete velocities $\boldsymbol{\xi}_q$. Solution for the discrete distributions is provided by assuming that each moment relaxes toward its equilibrium value $\hat{f}_m^{eq}$ at a rate specified by an associated relaxation parameter λ_m. The form of the equilibrium moments $\hat{f}_q^{eq}$, transformation matrix $M_{q,m}$, and inverse transformation matrix $M_{q,m}^*$ follow d'Humiéres and Ginzburg (d'Humiéres et al., 2002). This corresponds to solution of the equation:

$$f_q(\mathbf{x}_i + \boldsymbol{\xi}_q, t+1) - f_q(\mathbf{x}_i, t) = \sum_{m=0}^{18} M_{q,m}^* \lambda_m \left(\hat{f}_m^{eq} - \hat{f}_m \right) + F_q, \tag{19}$$

where $M_{q,m}^*$ are coefficients of the transformation matrix inverse and F_q is a contribution due to an external force $\mathbf{g}$:

$$F_q = w_q \rho_0 \boldsymbol{\xi}_q \cdot \mathbf{g} \tag{20}$$

The constant reference density ρ_0 is set to unity and the weights $w_0 = 1/3$, $w_q = 1/18$ for $q = 1, \ldots, 6$ and $w_q = 1/36$ for $q = 7, \ldots, 18$. The set of relaxation parameters are chosen to minimize the dependence of permeability on fluid viscosity (Pan, Luo and Miller, 2006):

$$\lambda_1 = \lambda_2 = \lambda_9 = \lambda_{10} = \lambda_{11} = \lambda_{12} = \lambda_{13} = \lambda_{14} = \lambda_{15} = \frac{1}{\tau}, \tag{21}$$

$$\lambda_3 = \lambda_6 = \lambda_8 = \lambda_{16} = \lambda_{17} = \lambda_{18} = \frac{8(2-\lambda_1)}{8-\lambda_1}, \tag{22}$$

where the parameter $\tau > 0.5$ related to the kinematic viscosity of the fluid:

$$\mu = \frac{1}{3}\left(\tau - \frac{1}{2}\right). \tag{23}$$

To describe non-Darcy flow, a sequence of steady-state velocity fields are simulated within the generated media using specified values of Fo to drive the flow in the x direction. Once a steady state velocity field has been reached for a given value of Fo, the macroscopic flow velocity $\mathbf{v}^{\oplus}$ is calculated using a density-weighted volume average of the pore-scale velocity field $\mathbf{u}(\mathbf{x}_i)$ integrated over the flow domain Ω_w:

$$\mathbf{v}^{\oplus} = \frac{\int_{\Omega_w} \rho_w \mathbf{v}_w dr}{\int_{\Omega_w} \rho_w dr} = \langle \mathbf{v}_w \rangle_{\Omega_w, \Omega_w, \rho_w} \tag{24}$$

The macroscopic velocity is used to compute the Reynolds number as defined by Eq. 2. Once the sequence of Fo values and their associated Reynolds numbers have been computed, Eq.4 is used to calculate the permeability and inertial coefficients associated with the analyzed media.

Results and Discussion

Non-Darcian flow simulations were performed by running the lattice Boltzmann simulator on the Topsail computing system, a Linux based cluster owned and operated by the University of North Carolina. The cluster is composed of 520 computing nodes, each equipped with 2 Intel quad-core processors (Model E5345/Clovertown) running at 2.3 GHz and 12 GB of memory. To reduce simulation times, the model was ran in parallel on 64 Topsail cores using Message Passage Interface (MPI).

Table 1: Generated Media

Lognormal Distributed Variance, σ^2	Porosity Range
0	0.38-0.60
0.1	0.35-0.54
0.2	0.32-0.48
0.3	0.30-0.42

Flow simulations were performed in systems of spheres with lognormal distributed radii of

variances, σ^2, 0, 0.1, 0.2, and 0.3 over a range of porosities, see Table 1. Within each porosity range, a sphere packing was generated for every increment of 0.01. To achieve stability, each of the packings had mean coordination numbers ≥ 6. To ensure the evolution of a porous continuum, each porous media system used within the simulations was a microscale representative elementary volume (REV) of a macroscopic system.

Development of Representative Elementary Volumes

The REV has to be large enough to capture the macroscale physics of concern, therefore the non-Darcy curve must be independent of both the lattice size of the simulated domain and the pore size of the generated media. To develop a porous medium that yielded grid-independent results, a system containing a set number of spheres was packed and the lattice size was increased until the non-Darcy curve converged to one definitive solution. To extend this system to a domain independent of pore structure, the number of spheres was incrementally increased until once again a definitive solution for the non-Darcy curve was reached. The relative intrinsic permeability and the inertial coefficients are shown as functions of sphere number for each variance of lognormal distributed radii in Fig.1.

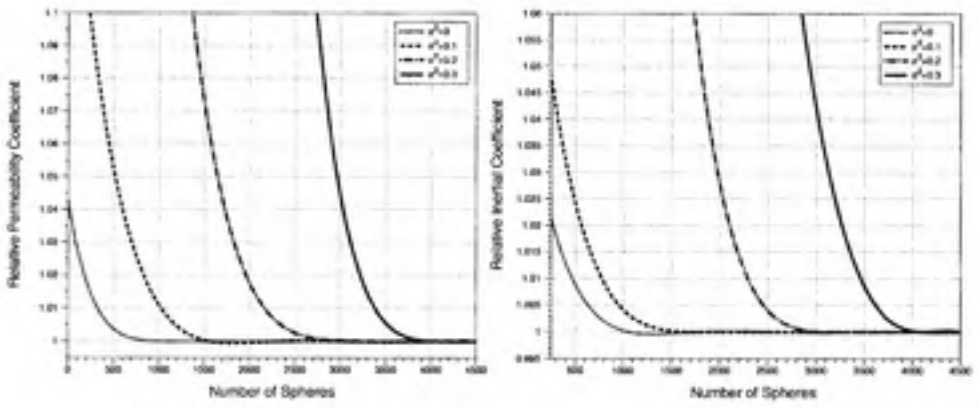

(a) Permeability (b) Inertial

Figure 1: Coefficient values relative to the associated REV values obtained for the permeability and inertial parameters for a range of sphere packings.

Table 2 outlines the number of spheres and cubic lattice sizes that were used to generate a REV porous medium for each variance of the log-normally distributed radii considered within the simulations.

Derived Correlations

Permeability Correlation

Existing correlations for the dimensionless permeability were compared to results obtained based on simulations performed using the lattice Boltzmann method. Points obtained from simulation did not adequately fit any of the functional forms describe in the background section for the full rangeof porosity values considered.

Fig. 2 shows how the Ergun relation deviated significantly from the simulation results for the full range of porosites, especially at higher porosity values (≥ 0.42). The Ergun relation deviation was qualitatively based on a straight tube geometry of the pore space and has been found to be valid only in a range of Reynolds numbers, $0 \leq \mathrm{Re} \leq 75$ (Ergun, 1952; Macdonald F., 1979). Based on the packing parameters set by the REV calculations (Table 2), the range of Reynolds numbers achieved within the simulation differs for each variance. The Reynolds number range is $0 \leq \mathrm{Re} \leq 140$ for the homogenous packing ($\sigma^2 = 0$), $0 \leq \mathrm{Re} \leq 130$ for $\sigma^2 = 0.1$, $0 \leq \mathrm{Re} \leq 115$ for $\sigma^2 = 0.2$, and $0 \leq \mathrm{Re} \leq 95$ for $\sigma^2 = 0.3$. As the Reynolds number range for each variance increases passed the upper limit of the Ergun relation, the difference between the permeability values from the simulation and those predicted by Ergun increases.

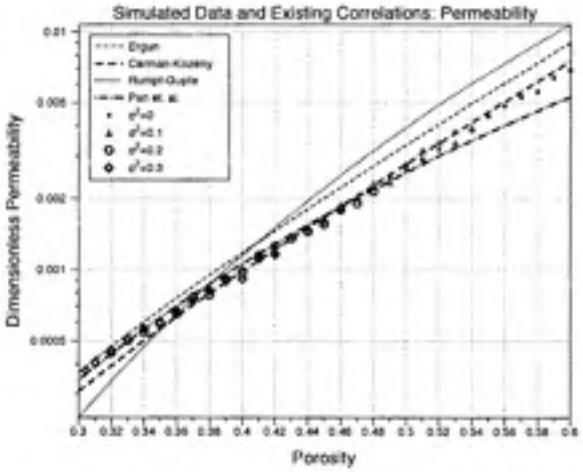

Figure 2: Comparison between the simulated data and the existing empirical relations.

Pan et al. based their permeability relation on a set of flow simulations with a porosity range of $0.33 \leq \epsilon \leq$ to 0.45 (Pan, Hilpert and Miller, 2001), correlating to the range of porosities the

Table 2: Representative Elementary Volumes for Generated Media

Variance, σ^2	Number of Spheres, N_s	Lattice Dimensions, n^3	Mean pixels per grain diameter, D
0	1500	360^3	32.84
0.1	1500	380^3	30
0.2	3000	460^3	27.577
0.3	4000	460^3	24.889

relation corresponds to the simulated data in Fig. 2. At the porosities outside the experimentally supported range, the Pan et al. relation underestimates the measured permeabilities.

The Carmen-Kozeny relation fit well to a range of the measured permeabilities, but for lower porosities ($\leq$ 0.42) the relation starts to veer off significantly from the data (Fig. 2). The lower porosity deviations are consistant with the findings of others (Pan, Hilpert and Miller, 2001) and have been attributed to the Carmen-Kozenzy relation only being valid for laminar flow (Prieur Du Plessis and Masliyah, 1991), an idea supported by the inertial parameter results from the simulation data. Fig. 4 shows how the inertial correction to Darcy's law, coefficient $\hat{b}$, for the simulated flow increases as porosity decreases. The deviation from Darcy flow at the lower porosity range subsequently decreases the validity of the Carmen-Kozeny relation.

The Rumpf-Gupte relation deviates the most from the simulated data, overpredicting the data for porosities $\geq$ 38 and underpredicting for porosities $\leq$ 38. The data for Rumpf-Gupte is based on sphere packings with relative standard deviations of the sphere-size distribution, $\tilde{\sigma}_D$, of 0.0945, 0.32, and 0.327 over a wide range of porosity (0.366 $\leq \epsilon \leq$0.64) and Reynolds number ($0 < Re < 100$) (Macdonald F., 1979). The $\sigma^2 = 0.3$ data within $0.36 < \epsilon < 0.42$ is the only simulation data that fits within the experimentally supported regime of the Rumpf-Gupte relation. Fig. 2 shows how the data within the Rumpf-Gupte experiments correlates to the porosity range where deviations are a minimum, an observation supported by (Pan, Hilpert and Miller, 2001).

An exponential fit of the full range of simulation data yielded more satisfactory agreement with the simulated data. The associated functional form is:

$$\hat{a}_1(\epsilon) = \alpha e^{\gamma\epsilon}, \tag{25}$$

where the best-fit coefficient values are $\alpha = 1.945 \times 10^{-5}$ and $\gamma = 9.846$. Fig. 3 compares the proposed correlation model to the simulated data.

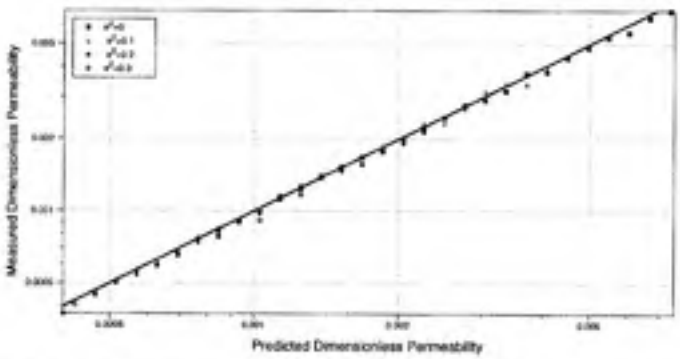

Figure 3: The proposed permeability correlation predicts the simulation data.

Inertial Correlation

Simulated values for the inertial parameter are shown in comparison with values predicted by Eq. 8 in Fig 4. Neither of the coefficients predicted by Ergun and Macdonald for the Ergun functional form (Eq. 8) provide a satisfactory fit to the simulation data, and both relations overpredict the lower range of porosities (< 0.40) and underpredict the higher range of porosities (> 0.40).

As discussed within the last section for the permeability coefficient, the range of tested Reynolds number seems to be a source of error between the simulated data and those predicted by the Ergun relation. The Ergun relation has also been found to be valid only in porosities ranging $0.38 \leq \epsilon \leq 0.47$ (Happel and Brenner, 1965), correlating to the range of data where the Ergun relation starts to converge with the simulated data before diverging at a porosity of 0.35.

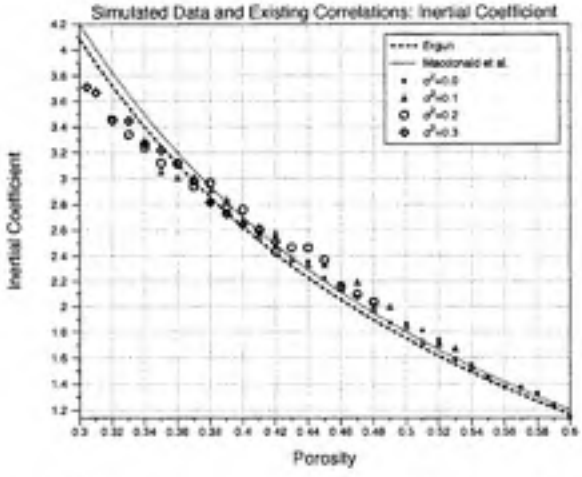

Figure 4: Comparison between the simulated data and the existing empirical relations.

The Macdonald et al. relation is the Ergun relation (Eq. 8) with a modified B coefficient based on the comparative analysis of numerous experimental results, including Rumpf-Gupte. The analysis also took in account data from a wide range of porosities ($0.123 \leq \epsilon \leq 0.919$) and granular shapes and sizes with the goal of deriving an Ergun relation that was applicable for packings of non-spherical grains (Macdonald F., 1979). Much of the lower porosity data ($\epsilon \leq 40$) came from experiments using irregular shaped objects, sand and gravel mixtures, and a variety of undisclosed materials. Since the simulated data only takes in account porous media composed of smooth spheres, roughness could explain the large deviations between the inertial parameter predicted by the Macdonald et al relation and the simulated data at porosities ≤ 40.

To provide a better fit for the full range of simulated data, non-linear least squares was used

to find the best fit coefficients to a generalized form of the Ergun relation:

$$\hat{b}_1(\epsilon) = B\frac{(1-\epsilon)^{\gamma_1}}{\epsilon^{\gamma_2}}. \tag{26}$$

where the coefficients are $B = 4.21$, $\gamma_1 = 1.58$ and $\gamma_2 = 0.38$. Fig. 5 compares the proposed correlation model to the simulated data.

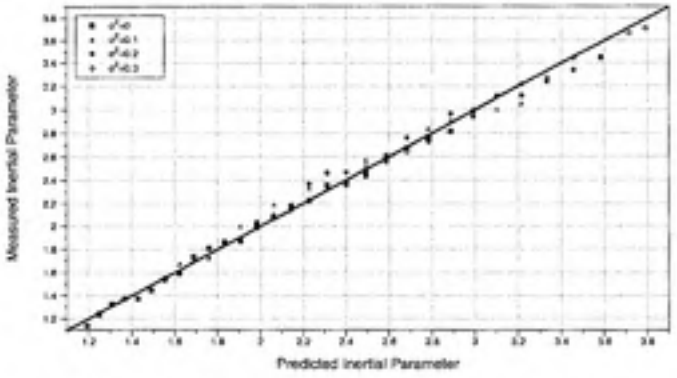

Figure 5: The proposed inertial correlation predicts the simulation data.

Conclusions

1. The full set of simulation data from the lattice-Boltzmann model did not fit any of the existing permeability correlations, the Ergun and Rumpf-Gupte relations over predict much of the porosity range while the Pan et al. and Carmen-Kozeny relations fit data within certain porosity ranges. It was observed that the deviations of the simulation data from the Pan et al. and Rumpf-Gupte relations correspond to the range of porosity values lacking experimental support where as the differences with the Carmen-Kozeny relate to the increase of the inertial parameter. It was also noted that as the Reynolds number increased past the validation range for the Ergun relation, the difference between the measured permeability and the Ergun predicted permeability grew. An exponential correlation model dependent on porosity was derived for the data set.

2. The inertial parameters from the flow simulations fit the generalized form of the Ergun relations but not any of the existing coefficients proposed by Ergun and Macdonald. A generalized form of Ergun's expression was constructed to provide a more satisfactory fit of the simulated data.

References

Bear, J. 1972. *Dynamics of Fluids in Porous Media*. New York: Elsevier.

d'Humiéres, D., I. Ginzburg, M. Krafczyk, P. Lallemand and L. S. Luo. 2002. "Multiple-relaxation-time lattice Boltzmann models in three dimensions." *Philosophical Transactions of the Royal Society of London Series A-Mathematical Physical and Engineering Sciences* 360:437–451.

Ergun, S. 1952. "Fluid flow through packed columns." *Chemical Engineering Progress* 48:89–94.

Fourar, M., G. Radilla, R. Lenormand and C. Moyne. 2004. "On the non-linear behavior of a laminar single-phase flow through two and three-dimensional porous media." *Advances in Water Resources* 27(6):669–677.

Geertsma, J. 1974. "Estimating the coefficient of inertial resistance in fluid flow through porous media." *Soc. Petrol. Eng.* pp. 211–216.

Gray, W. G. and C. T. Miller. 2006. "Thermodynamically Constrained Averaging Theory Approach for Modeling Flow and Transport Phenomena in Porous Medium Systems: 3. Single-Fluid-Phase Flow." *Advances in Water Resources* 29(11):1745–1765.

Happel, J. and H. Brenner. 1965. *Low Reynolds Number Hydrodynamics*. NJ: Prentice-hall, Englewood Cliffs.

Hassanizadeh, S. M. and W. G. Gray. 1987. "High-Velocity Flow in Porous-Media." *Transport in Porous Media* 2(6):521–531.

Hassanizadeh, S. M. and W. R. Gray. 1988. "Reply to Comments by Barak on 'High Velocity Flow in Porous Media' by Hassanizadeh and Gray." *Transport in Porous Media* 3(3):319–321.

Ma, H. and D. W. Ruth. 1994. "A Numerical-Analysis of the Interfacial Drag Force for Fluid-Flow in Porous-Media." *Transport in Porous Media* 17(1):87–103.

Macdonald F., El-Sayed S., Mow K. Dullien F. 1979. "Flow through Porous Media - the Ergun Equation Revisited." *Ind. Eng. Chem. Fundam.* 18(3):199–208.

McClure, J. E., W. G. Gray and C. T. Miller. 2010. "Beyond Anisotropy: Examining Non-Darcy Flow in Asymmetric Porous Media." *Transport in Porous Media* 84(2):535–548.

Pan, C., L.-S. Luo and C. T. Miller. 2006. "An evaluation of lattice Boltzmann schemes for porous medium flow simulation." *Computers & Fluids* 35(8–9):898–909.

Pan, C., M. Hilpert and C. T. Miller. 2001. "Pore-scale modeling of saturated permeabilities in random sphere packings." *Physical Review E* 64(6):9.

Panfilov, M. and M. Fourar. 2006. "Physical splitting of nonlinear effects in high-velocity stable flow through porous media." *Advances in Water Resources* 29(1):30–41.

Prieur Du Plessis, J. and J. H. Masliyah. 1991. "Flow Through Isotropic Granular Poros Media." *Transport in Porous Media* 6:207–221.

Rumpf, H. and A. R. Gupte. 1971. "Einflüsse der Porosität und Korngrössenverteilung im Widerstandsgesetz der Porenströmung." *Chemie Ingenieur Technik* 43:367–375.

Tek, M.R. 1957. "Development of a generalized Darcy equation." *Trans AIME* 210:376–377.

Wang, X., F. Thauvin and K. K. Mohanty. 1999. "Non-Darcy flow through anisotropic porous media." *Chemical Engineering Science* 54(12):1859–1869.

Williams, S. and A. Philipse. 2003. "Random packings of spheres and spherocylinders simulated by mechanical contraction." *Physical Review E* 67.